the polypeptides linking the binding domain to the channel domain are rotated 45° clockwise in one subunit pair but 45° counterclockwise in the other pair. In this issue of *Neuron*, Sobolevsky et al. (2004), provide data that extend this idea and suggest that the upper third of the channel domain, like the glutamate binding domain, assumes a 2-fold rotational symmetry. Therefore, the transition to 4-fold symmetry, if at all, occurs deeper in the membrane (gray dotted line, Figure 1B).

Building on previous studies where they have mutated the pore-facing residues in transmembrane domain M3 to cysteine, Sobolevsky et al. tested whether any of these sites can react with Cd^{+2} or the oxidizing agent copper(II):phenanthroline. Their working hypothesis was that only closely positioned cysteines can be bridged by Cd^{2+} or form a disulfide bond and thus block the pore. A blocking effect produced only in the presence of glutamate suggests that the reacting cysteines are separated from each other in the closed state but come together in the open state. Indeed, the authors found that channels incorporating a cysteine in a position located at the upper third of M3 behaved in this manner. The authors then coexpressed the cysteine-substituted subunit with a wild-type subunit in various ratios and fitted the blocking effects produced by either reagent to various models of mutant to wild-type spatial rearrangements. The data were best fitted with a model in which the reacting cysteines are placed one across from the other in a 2-fold rather than a 4-fold symmetric manner. Such an organization fits the 2-fold dimer-of-dimer arrangement of the glutamate binding domains. Based on this similarity, the authors suggested that Cd^{2+} binding and cross-linking occurs between two pairs of adjacent subunits arising from different dimers (red/green and blue/yellow M3s; Figure 1). To accommodate their findings to previous models incorporating a 4-fold symmetric pore (formed mainly by M2; Figure 1), the authors introduced opposite 45° bends in the upper third of M3 in each dimer (Figure 1B; the level of gray dotted line). In this way, the bent M3 from one dimer can approach the M3 of the lateral dimer upon gating.

The models for the glutamate binding domain and the ion channel, when combined, have some interesting features. First, the binding domain model predicts a compression in the vertical dimension upon binding glutamate (Figure 1B, vertical black arrows on the right side of the binding domain). The model for the pore-forming regions M2-M3 predicts that with channel opening the transmembrane domain also compresses in the vertical dimension because of the bend of M3 helices. Therefore, one can speculate that during gating the binding domain may move up and down relative to the channel, being closer in the open state. Second, the M2-M3 model predicts that, during gating, the outer part of the channel rotates counterclockwise upon channel opening (black arrows, Figure 1B, middle). Therefore, the binding domains as a unit (or only the D2s, as shown in Figure 1C, middle) may also follow this rotation. Alternatively, the binding domain stays in place while the polypeptide linkers rotate (not shown). As more tension is put on these regions, the linkers may rapidly rotate back, thus accelerating channel entry into the desensitized state. It should be noted that S1S2 crystallized much better when these linkers were removed from the original S1S2 construct (Mayer and Armstrong, 2003), implying a large degree of structural flexibility in this region. Obviously, answers await the availability of crystals made of the intact receptor, and preferably in each of the three basic conformations: resting, active, and desensitized.

Yael Stern-Bach
The Institute of Basic Dental Science
The Hebrew University-Hadassah School of Dental Medicine
Jerusalem 91120
Israel

Selected Reading

Ayalon, G., and Stern-Bach, Y. (2001). Neuron *31*, 103–113.

Barry, M.F., and Ziff, E.B. (2002). Curr. Opin. Neurobiol. *12*, 279–286.

Dingledine, R., Broges, K., Bowie, D., and Traynelis, S.F. (1999). Pharmacol. Rev. *51*, 7–61.

Greger, I.H., Khatri, L., Kong, X., and Ziff, E.B. (2003). Neuron *40*, 763–774.

Horning, M.S., and Mayer, M.L. (2004). Neuron *41*, this issue, 379–388.

Mayer, M.L., and Armstrong, N. (2003). Annu. Rev. Physiol. Published online September 8, 2003. 10.1146/annurev.physiol.66.050802.084104.

Rosenmund, C., Stern-Bach, Y., and Stevens, C.F. (1998). Science *280*, 1596–1599.

Sobolevsky, A.I., Yelshansky, M.V., and Wollmuth, L.P. (2004). Neuron *41*, this issue, 367–378.

Sun, Y., Olson, R., Horning, M., Armstrong, M., Mayer, M., and Gouaux, E. (2002). Nature *417*, 246–253.

Vesicle Priming and Depriming: A SNAP Decision

Synapses have a limited pool of vesicles that are docked and primed for rapid release. In neuroendocrine cells, splice variants of the SNARE protein SNAP-25 and phosphorylation of SNAP-25 independently influence the size of the releasable vesicle pool, possibly by altering the rate of vesicle depriming. Pre- and posttranslational modifications of SNAP-25 may therefore affect synaptic strength.

An important presynaptic determinant of synaptic efficacy is the number of synaptic vesicles available for release. Such releasable vesicles—generally a small subset of all the vesicles in a presynaptic ending—are in contact with the plasma membrane and have undergone all the preparatory steps necessary for rapid membrane fusion. Changes in the size of this releasable pool of vesicles can contribute to synaptic plasticity, such as depression and facilitation. In this issue of *Neuron*, Nagy et al. (2004) explore the molecular mechanisms regulating the size of the releasable pool in adrenal chromaffin cells, a well-characterized neuroendocrine model for calcium-dependent exocytosis. They show

that cAMP-dependent protein kinase (PKA) strongly affects the size of releasable vesicle pools, in part by phosphorylating the SNARE protein SNAP-25, and that pool size is also influenced by the particular SNAP-25 splice variant expressed. Surprisingly then, both post-translational (phosphorylation) and pretranslational (alternative splicing) modifications of the same molecule, SNAP-25, regulate the number of vesicles available for release.

To separate the intertwined effects of cAMP and Ca^{2+}, Nagy and colleagues employed the photolyzable Ca^{2+} chelator NP-EGTA, which held basal internal Ca^{2+} constant and thus controlled for cross talk between cAMP and basal Ca^{2+}. They then triggered exocytosis by photolytic release of Ca^{2+} from NP-EGTA, bypassing the confounding effects of cAMP on Ca^{2+} channel gating and Ca^{2+} entry. Exocytosis was monitored using membrane capacitance measurements and validated by simultaneous amperometric measurement of catecholamine release. This combination permits detailed kinetic analysis of the exocytotic response and allows PKA-dependent modulation of the release process to be distinguished from modulation of the number of vesicles available for release. After photolysis of NP-EGTA, the secretory response in chromaffin cells typically consists of a rapid burst as the releasable vesicles fuse, followed by sustained release attributed to fusion of reserve vesicles as they refill the releasable pool during the prolonged postflash elevation of $[Ca^{2+}]_i$. The burst has two kinetic components, representing parallel fusion of vesicles in a rapidly releasable pool (RRP; $\tau \approx 30$ ms) and a slowly releasable pool (SRP; $\tau \approx 300$ ms). The RRP is thought to be refilled from the SRP (Voets et al., 1999), leading to a linear maturation scheme shown in Figure 1.

Nagy and coworkers used a combination of pharmacology and phosphorylation mutants of SNAP-25 to show that PKA-dependent phosphorylation of SNAP-25 increases the size of the SRP, without changing the kinetics of vesicle fusion or the sustained release representing pool refilling. PKA activity also increased the size of the RRP, again without altering fusion rate. However, this action was not affected by phosphorylation mutants of SNAP-25 and therefore involves an as yet unknown target (see Figure 1). Thus, PKA regulated the size of both releasable pools but not the fusion step itself. By what mechanism does PKA's phosphorylation of SNAP-25 increase the size of SRP? In light of the linear maturation scheme shown in Figure 1, one hint comes from the finding that sustained release was unaffected by manipulations that alter PKA-dependent phosphorylation. If sustained release indeed represents the movement of reserve vesicles into the primed releasable pool, then failure of PKA inhibitors or SNAP-25 phosphorylation mutants to affect the sustained component indicates that the rate of vesicle priming is not altered by SNAP-25 phosphorylation. In turn, this implies that the target must therefore be the rate of vesicle *depriming* (i.e., the stability of primed vesicles). So, Nagy and coworkers proposed that depriming is reduced when SNAP-25 is phosphorylated and enhanced when SNAP-25 is dephosphorylated, leading to the observed PKA-dependent changes in size of the SRP. This proposal represents a novel and unsuspected role for a SNARE protein in stabilizing primed vesicles.

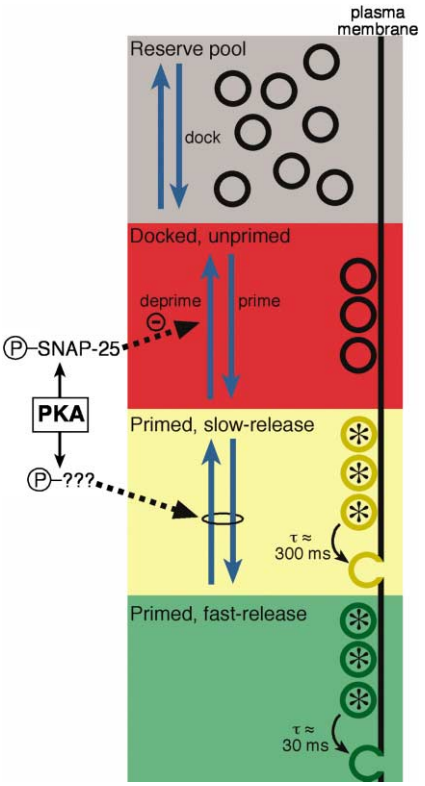

Figure 1. Vesicle Pools in Adrenal Chromaffin Cells

Asterisks indicate vesicles that are primed for Ca^{2+}-triggered fusion. PKA = protein kinase A.

Another important result was that the size of the exocytotic burst was affected by the splice variant of SNAP-25 that was expressed in the chromaffin cells (Sørensen et al., 2003). SNAP-25 exists in two forms, a and b, differing by nine amino acids as a result of alternative RNA splicing. Chromaffin cells normally express the a form, whereas the b form dominates in the brain. Overexpression of SNAP-25b in chromaffin cells more than doubled both components of the exocytotic burst relative to wild-type controls (i.e., expressing SNAP-25a), with no change in the fusion kinetics or the sustained component. Superimposed on this larger pool size, PKA-dependent phosphorylation of SNAP-25b affected the releasable pool in just the same way as with the SNAP-25a form. Thus, for both splice variants, phosphorylation by PKA regulates the relative size of the exocytotic burst, but the baseline size of the releasable pools is determined independently by the particular splice variant of SNAP-25.

Neurons, like chromaffin cells, exhibit multiple kinetic components of release, although the rates are about 10-fold faster than in chromaffin cells (e.g., Mennerick and Matthews, 1996; Sakaba and Neher, 2001). If the fastest component of neuronal exocytosis is analogous to the RRP of chromaffin cells, then the number of synaptic vesicle available for rapid release might be controlled by the actions of PKA on an unidentified target. Whether neurons have a pool analogous to the SRP is not known; the slower releasable pool in neurons may simply indicate a greater distance from Ca^{2+} channels

or differences between active zones. However, the high degree to which SNARE protein function is conserved suggests that the phosphorylation state of SNAP-25 also regulates the transition between distinct vesicle pools in neurons, although the details of these pools may differ. For example, PKA-dependent SNAP-25 phosphorylation may regulate the rate of vesicle depriming from the neuronal RRP. It is worth noting that the rate of depriming is significantly slower in synaptic terminals of bipolar neurons than in chromaffin cells (Heidelberger et al., 2002). In light of the results of Nagy et al., one possibility is that the balance between phosphorylation and dephosphorylation favors the phosphorylated state in the bipolar neuron. Given the relationship between the neuronal RRP and synaptic efficacy, confirmation of the role of SNAP-25 and the identification of other factors that regulate pool size in neurons, such as the unidentified target of PKA activity, should be given high priority.

Ruth Heidelberger[1] and Gary Matthews[2]
[1]Department of Neurobiology and Anatomy
University of Texas Medical School at Houston
Houston, Texas 77030
[2]Department of Neurobiology and Behavior
State University of New York
Stony Brook, New York 11794

Selected Reading

Heidelberger, R., Sterling, P., and Matthews, G. (2002). J. Neurophysiol. *88*, 98–106.

Mennerick, S., and Matthews, G. (1996). Neuron *17*, 1241–1249.

Nagy, G., Reim, K., Matti, U., Brose, N., Binz, T., Rettig, J., Neher, E., and Sørensen, J.B. (2004). Neuron *41*, this issue, 417–429.

Sakaba, T., and Neher, E. (2001). Neuron *32*, 1119–1131.

Sørensen, J.B., Nagy, G., Varoqueaux, F., Nehring, R.B., Brose, N., Wilson, M.C., and Neher, E. (2003). Cell *114*, 75–86.

Voets, T., Neher, E., and Moser, T. (1999). Neuron *23*, 607–615.

Design for a Binary Synapse

The mammalian rod transfers a binary signal, the capture of 0 or 1 photon. In this issue of *Neuron*, Sampath and Rieke show in mouse that the rod's tonic exocytosis in darkness completely saturates a G protein cascade to close nearly all postsynaptic channels. A full-sized photon event supresses exocytosis sufficiently to allow ~30 postsynaptic channels to open simultaneously. Thus, the synapse behaves like a digital gate, whose hallmark is reliability and resistance to noise.

Although we generally consider the human visual system as specialized for daylight, roughly 95% of our photoreceptors are rods, and in this respect we resemble the mouse. Rods dominate the photoreceptor sheet (outside the all-cone fovea), because from dusk till dawn, natural light provides less than one photon capture per rod over its integration time. The rod's transducer responds to a single photon capture by hyperpolarizing ~1 mV, a response that rises modestly above the noise (Baylor et al., 1984; Schneeweis and Schnapf, 1995; Field and Rieke, 2002). Such single-photon detectors must pack densely in order to maximize the photon catch and produce overall images whose quality is approximated in Figure 1A. But we would see such images only if most of the information embodied by the patterns of single photon capture actually reached the brain. That they do arrive is certain because a photon event reliably evokes several spikes in a ganglion cell (Barlow et al., 1971); however, there are serious obstacles—especially at the initial synapse onto the bipolar cell dendrite.

First, the rod's single-photon current in varies in amplitude (Figure 1B, upper trace). If it rises 5-fold above the noise, the event is easily spotted, but when it is much smaller, as occurs commonly in the mouse rod, the event can easily be taken for noise (Field and Rieke, 2002). Second, while this rod is producing a marginal photon signal, 19 other rods also contact the same bipolar cell and potentially contribute intrinsic noise (from their phototransduction cascades) and also synaptic noise (from their poisson vesicle release). Third, glutamate binding to a metabotropic receptor on the bipolar dendritic tip tonically activates a G protein cascade that closes cation channels in the dark. Fluctuations in this cascade could potentially cause fluctuations in the number of channels closed in the dark or open in light. This would contribute postynaptic noise at each of 20 sites—that would accumulate at the bipolar soma and swamp the photon response from one rod.

A solution was proposed: let the initial synapse amplify nonlinearly to boost the larger voltages (likely to be photon events) more than smaller voltages (likely to be noise) (Baylor et al., 1984; van Rossum and Smith, 1998). This conjecture was proved by Field and Rieke (2002), who demonstrated in the bipolar cell that nonlinear amplification of single photon events strongly rejects noise and, along with it, the smaller single photon events. Sampath and Rieke (2004) now address the next big question: what causes this nonlinear amplification?

Their assay was technically difficult, requiring them to slice a mouse retina in the dark (using infrared goggles) and then record the photocurrent from a tiny bipolar cell body without disturbing its delicate synaptic input from the rods. Nonlinearity was assessed by the Hill exponent, which expresses the relation between stimulus intensity and response. The relation is linear when the exponent is 1. Under these conditions, and using flash strengths somewhat greater than 1 photoisomerization (Rh*) per rod, the Hill coefficient was typically ~1.5, indicating "supralinearity," i.e., bigger responses are amplified more (Field and Rieke, 2002). Sampath and Rieke first tested whether feedback from interneurons, such as a horizontal cell that integrates input from about 1000 rods (Figure 1C; Nelson et al., 1975), causes the nonlinearity. They blocked all potential feedback by applying antagonists of AMPA and NMDA glutamate receptors that excite these interneurons. The Hill coefficient was unaffected, showing that supralinearity at these intensities is not caused by feedback and must be intrinsic to the synapse between rod and bipolar dendrite.